

# Erlotinib, an Effective Epidermal Growth Factor Receptor Tyrosine Kinase Inhibitor, Induces p27<sup>KIP1</sup> Up-Regulation and Nuclear Translocation in Association with Cell Growth Inhibition and G<sub>1</sub>/S Phase Arrest in Human Non-Small Cell Lung Cancer Cell Lines

Yi-He Ling, Tianhong Li, Ziqiang Yuan, Missak Haigheer, Thomas K. Weber, and Roman Perez-Soler

Departments of Oncology (Y.H.L., T.L., M.H., R.P.-S.) and Molecular Genetics (Z.Y., T.K.W.), Albert Einstein College of Medicine, Bronx, New York

Received February 6, 2007; accepted April 23, 2007

## ABSTRACT

Erlotinib, a small-molecule epidermal growth factor receptor (EGFR) tyrosine kinase inhibitor, has been shown to have potent antitumor effects against human non-small cell lung cancer (NSCLC) cell growth; however, the mechanism of such an effect is not elucidated. Here, we demonstrate that erlotinib-induced cell growth inhibition in EGFR-expressing human H322 NSCLC cells was accompanied by G<sub>1</sub>/S phase arrest, which was largely caused by decrease in expression of G<sub>1</sub>/S-related cyclins, suppression of activities of cyclin-dependent kinase (CDK) 2 and CDK4, induction of CDK inhibitor p27<sup>KIP1</sup>, and retinoblastoma phosphorylation. To further understand the role of p27<sup>KIP1</sup> in G<sub>1</sub>/S arrest and cell growth inhibition by erlotinib, we determined its effect on the expression of p27<sup>KIP1</sup> at transcriptional and posttranscriptional levels. Studies using real-time reverse transcription-polymerase chain reaction analysis and p27 promoter-driven luciferase reporter show that erlotinib treatment resulted in the promotion of

gene transcription. In addition, erlotinib treatment led to an increase in p27<sup>KIP1</sup> half-life by inhibiting p27<sup>KIP1</sup> phosphorylation at Thr187 and by down-regulating Skp2 expression. Furthermore, immunofluorescence staining and cell fractionation showed that erlotinib treatment induced p27<sup>KIP1</sup> translocation to the nucleus. Knockdown of p27<sup>KIP1</sup> expression with p27<sup>KIP1</sup> small interfering RNA significantly abrogated erlotinib-induced G<sub>1</sub> phase arrest and cell growth inhibition, suggesting that induction of p27<sup>KIP1</sup> is required for G<sub>1</sub> arrest and cell growth inhibition by erlotinib. It is noteworthy that we found that G<sub>1</sub> arrest and p27<sup>KIP1</sup> up-regulation by erlotinib occurred in the sensitive cell lines but to a lesser extent in the resistant cell lines. Taken together, these results suggest that erlotinib inhibits human NSCLC cell growth predominantly by inducing p27<sup>KIP1</sup> expression and by suppressing cell-cycle events in the G<sub>1</sub>/S transition.

Cell cycle control plays a fundamental role in cell differentiation, proliferation, and cell growth. The proper regulation of the cell cycle machinery, including cyclins, cyclin-dependent kinases (CDKs), and CDK inhibitors, is essential for control of cell growth (Matsushima et al., 1991; Bellapenna et al., 1998).

This work was supported by National Institutes of Health grants CA91784 and CA96515 and by OSI Pharmaceuticals, Inc. Article, publication date, and citation information can be found at <http://molpharm.aspetjournals.org>. doi:10.1124/mol.107.034827.

Several lines of evidence have demonstrated that growth factors trigger cascades of intracellular signals that lead to activation of nuclear transcriptional factors that activate cyclin/CDK complexes; active cells pass the G<sub>1</sub> checkpoint and embark on DNA replication in S phase (Matsushima et al., 1991). G<sub>1</sub>/S transition is positively controlled by two families of CDKs, including the complexes of CDK2/cyclin E and cyclin A or the complexes of CDK4/cyclin D or CDK6/cyclin D. In contrast, the complexes of CDK inhibitors can be subdivided into two families, including the INK4 family, consisting

**ABBREVIATIONS:** CDK, cyclin-dependent kinase; BrdU, bromodeoxyuridine; CIP, cyclin inhibitory protein; KIP, kinase inhibitory protein; EGFR, epidermal growth factor receptor; FACS, fluorescence-activated cell sorting; NSCLC, non-small-cell lung cancer; PAGE, polyacrylamide gel electrophoresis; Rb, retinoblastoma; RT-PCR, reverse transcription-polymerase chain reaction; siRNA, small interfering RNA; PI3, phosphatidylinositol 3; DMSO, dimethyl sulfoxide; MTT, 3-(4,5-dimethylthiazol-2-yl)-2,5-diphenyltetrazolium; PBS, phosphate-buffered saline; FITC, fluorescein isothiocyanate; DAPI, 4,6-diamidino-2-phenylindole; PKB, protein kinase B; ERK, extracellular signal-regulated kinase; LY294002, 2-(4-morpholinyl)-8-phenyl-1(4H)-benzopyran-4-one hydrochloride; U0126, 1,4-diamino-2,3-dicyano-1,4-bis(o-aminophenylmercapto)butadiene; AG1478, 4-(3'-chloroanilino)-6,7-dimethoxy-quinazoline.

of p16<sup>INK4a</sup>, p15<sup>INK4b</sup>, p18<sup>INK4c</sup>, and p19<sup>INK4d</sup> and KIP/CIP families consisting of p21<sup>WAF1/CIP1</sup>, p27<sup>KIP1</sup>, and p57<sup>KIP2</sup> (Sherr and Roberts, 1999). Other critical events for the G<sub>1</sub>/S transition are Rb protein phosphorylation and the release of its regulatory E2F proteins, which translocate to the nucleus and induce transcription of target genes that are required for cell proliferation (Weinberg, 1995; Dyson, 1998).

The epidermal growth factor receptor (EGFR) is a tyrosine kinase receptor of the ErbB family. Upon ligand binding, EGFR may either homodimerize or heterodimerize, resulting in transautophosphorylation (Yarden and Sliwkowski, 2001). The tyrosine-phosphorylated EGFR then served as a docking molecule to initiate the activation of downstream pathways, including the activation of PI3/AKT (promoting cell survival) and/or the activation of Raf/Ras/mitogen-activated protein kinase cascades (associated with cell proliferation) (Salomon et al., 1995). Moreover, EGFR and its family are implicated in the regulation of cell growth, transformation, and apoptosis (Klapper et al., 2000). Many tumor cells, especially epithelial cell-derived tumors, express elevated levels of EGFR or express mutant versions of ErbB family members. A number of reports have demonstrated high expression of EGFR in NSCLC cells (Haeder et al., 1988; Scagliotti et al., 2004). Because increased EGFR expression is known to correlate with poor clinical outcome in patients with NSCLC, the EGFR has been considered a potential therapeutic target. In recent years, several compounds have been developed that directly target the EGFR signaling pathway and have significant anticancer activity (Noonberg and Beer, 2000; Herbst and Bunn, 2003). Erlotinib (Tarceva; OSI-420; OSI Pharmaceuticals, Melville, NY) is an orally bioavailable quinazoline derivative that selectively inhibits the EGFR tyrosine kinase by competitively inhibiting the intracellular ATP binding domain and blocking signal transduction pathways implicated in cell proliferation and survival of cancers (Moyer et al., 1997; Pollack et al., 1999). Preclinical studies demonstrated erlotinib potent activity against tumor cell growth accompanied by increased EGFR activation. Erlotinib as a single agent has demonstrated significant clinical activity even in patients with NSCLC treated previously and has improved patient survival in a randomized placebo-controlled trial (Lynch et al., 2005), and recently it has been approved by the U.S. Food and Drug Administration as the second-line drug for treatment of patients with NSCLC. Although erlotinib has marked antitumor activity in both in vitro and in vivo systems, the mechanisms of its tumor effects remain to be elucidated. In this work, we used the erlotinib-sensitive human H322 NSCLC cell line as model to examine the effects of erlotinib on cell proliferation and cell cycle machinery. Our results demonstrate that erlotinib treatment causes cell cycle arrest at G<sub>1</sub>/S phase accompanied by a decline in the expression of G<sub>1</sub>-related regulators, remarkable suppression of CDK2 and CDK4 activities, and induction of CDK inhibitor p27<sup>KIP1</sup>. In addition, we found that erlotinib treatment resulted in Rb hypophosphorylation. Moreover, we found that erlotinib induces p27<sup>KIP1</sup> accumulation via promotion of p27<sup>KIP1</sup> transcription and protein stabilization. Erlotinib treatment resulted in p27<sup>KIP1</sup> translocation to the nucleus. Knockdown of p27<sup>KIP1</sup> expression with p27 siRNA caused abrogation of G<sub>1</sub> phase arrest and cell growth inhibition by erlotinib. It is noteworthy that we observed a direct relationship between G<sub>1</sub> phase arrest

and cell sensitivity to erlotinib in several human NSCLC cell lines. The results provide insights into the cell cycle effects of erlotinib and may be used as potential surrogate endpoints of drug action in clinical studies.

## Materials and Methods

**Chemicals.** Erlotinib was supplied by OSI Pharmaceuticals Inc., dissolved in DMSO (10 mM) as a stock solution, and diluted to the required concentration with RPMI 1640 medium. The following antibodies were used for immunoblot analysis: immunoprecipitation, and immunostaining monoclonal antibody to cyclin A (Upstate Biotechnology, Lake Placid, NY), monoclonal antibody to cyclin D1 (HD11; Santa Cruz Biotechnology, Inc., Santa Cruz, CA), and polyclonal antibody to cyclin D1 (D-120; Santa Cruz Biotechnology), monoclonal antibody to cyclin D2 (Ab-1; Calbiochem, La Jolla, CA), monoclonal antibody to cyclin E (Ab-1; Calbiochem), monoclonal antibody to CDK2 (D-12; Santa Cruz), and CDK4 (BD Pharmingen, Inc., San Diego, CA), monoclonal antibody to p21<sup>WAF1/CIP1</sup> (p21; Calbiochem), p27<sup>KIP1</sup> (F-8; Santa Cruz), and p16<sup>INK4a</sup> (50.1; Santa Cruz Biotechnology), monoclonal antibody to Rb, and polyclonal antibodies to Rb Ser795 and Ser780 (Cell Signaling Technology, Danvers, MA), monoclonal antibodies to E2F1 (K-10; Cell Signaling Technology), and polyclonal antibodies to SKP1 and p27<sup>KIP1</sup> (Santa Cruz Biotechnology), polyclonal anti-Sp1 antibody (p2; Santa Cruz Biotechnology), polyclonal antibodies to EGFR, p-EGFR, AKT, and p-AKT (Cell Signaling), and polyclonal antibodies to ERK and p-ERK (Pierce, Madison, WI). Other chemicals were obtained from Sigma Chemical Co. (St. Louis, MO).

**Cell Lines and Cell Culture.** Human non-small-cell lung cancer cell lines (H322, H358, A431, H1299, H596, and H1299), and human skin epidermoid carcinoma A431 cells were purchased from American Type Culture Collection (Manassas, VA). Human head and neck carcinoma cell line was a generous gift from OSI Pharmaceuticals (Farmingdale, NY). All cell lines were grown in RPMI 1640 medium with 10% fetal bovine serum in a humidified air atmosphere with 5% CO<sub>2</sub>.

**Cell Growth Assay.** Exponentially growing cells ( $2 \times 10^4$  cells/cell) were seeded on a 96-well plate overnight. After cell attachment, cells were treated to various concentrations of erlotinib at 37°C for 24 h. After exposure, cell survival fractions were assessed by viable cell count with trypan blue exclusion or by colorimetric assay based on the reduction of 3-(4,5-dimethylthiazol-2-yl)-2,5-diphenyltetrazolium bromide (MTT).

**Cell Cycle Assay.** H322 cells were exposed to various concentrations of erlotinib for 24 h or to 2 μM erlotinib for the indicated times. Cells were washed twice with cold PBS solution and harvested by trypsinization. After fixing with cold 75% ethanol overnight, cells were stained with 1 μg/ml propidium iodide and exposed to 5 μg/ml RNase I at room temperature for 3 h. The cell cycle distribution was assessed by FACS flow cytometer analysis (BD Biosciences, San Jose, CA). For determination of BrdU incorporation into DNA, cells were treated with 2 μM erlotinib for the indicated time, and then 10 μM BrdU was added into cell culture. After incubation for 1 h, the incorporated BrdU was detected with an FITC-BrdU assay kit according to the manufacturer's instruction (Calbiochem, Cambridge, MA).

**Immunoblot Analysis.** Cells were lysed with lysis buffer containing 50 mM Tris-HCl, pH 7.5, 150 mM NaCl, 1 mM EDTA, 1 mM EGTA, 1 mM NaF, 1 mM phenylmethylsulfonyl fluoride, 1 mM dithiothreitol, 20 μg/ml leupeptin, 20 μg/ml aprotinin, 0.1% Triton X-100, and 1% SDS at 0 to 4°C for 15 min. Equal amounts of lysates (50 μg of protein) were subjected to electrophoresis on either 7 or 12% SDS-PAGE. After electrophoresis, protein blots were transferred to a nitrocellulose membrane and probed with the corresponding primary antibodies. The detected protein signals were visualized by an enhanced chemiluminescence reaction system (GE Healthcare, Chalfont St. Giles, Buckinghamshire, UK).

**CDK Kinase Assay.** Cells were exposed to 2  $\mu\text{M}$  erlotinib for the indicated times and harvested by trypsinization. Cells were suspended in a lysis buffer on an ice-bath for 10 min. After centrifugation at 15,000g at 4°C for 10 min, the supernatant was collected for immunoprecipitation. Equal amounts of supernatant (500  $\mu\text{g}$  of protein) were incubated with 2  $\mu\text{g}$  of anti-CDK2 or anti-CDK4 antibodies and 25  $\mu\text{l}$  of protein A/G conjugated agarose beads at 0 to 4°C overnight. After washing three times with lysis buffer, immunoprecipitates were incubated at 30°C for 15 min in 30  $\mu\text{l}$  of reaction mixture containing 20 mM HEPES, pH 7.4, 10 mM *p*-nitrophenyl phenylphosphonate, 20 mM  $\text{MgCl}_2$ , 1 mM EDTA, 1 mM  $\text{Na}_2\text{VO}_4$ , 1  $\mu\text{M}$  ATP, 1  $\mu\text{Ci}$  of [ $\gamma$ - $^{32}\text{P}$ ]ATP (Amersham), and 5  $\mu\text{g}$  of histone H1 (Sigma) as a substrate for CDK2 assay or 5  $\mu\text{g}$  of Rb fusion protein (Cell Signaling) as a substrate for CDK4 assay. The reaction was terminated by the addition of 2 $\times$  SDS-PAGE sample buffer. After boiling for 5 min, the supernatants were collected by centrifugation at 15,000g for 5 min and then subjected to 12% SDS-PAGE. Activities of CDK2 and CDK4 were determined by autoradiography of the dried gels.

**Subcellular Fractionation.** Cells were treated with 2  $\mu\text{M}$  erlotinib or with the same volume of medium containing 0.1% DMSO as a control for 24 h, washed twice with ice-cold PBS solution, and harvested by trypsinization. Cells were suspended in an ice-cold nuclei isolation buffer containing 10 mM HEPES, pH 7.5, 1.5 mM  $\text{MgCl}_2$ , 10 mM KCl, 0.5 mM dithiothreitol, and 1% Triton X-100, and incubated on an ice-bath for 5 min. After centrifugation at 15,000g at 4°C for 5 min, the supernatant was collected as a cytosolic fraction. The pellets were resuspended in lysis buffer containing 1% SDS, and after incubation on an ice-bath for 5 min, the lysate was centrifuged, and supernatant was collected as a nuclear fraction. After determination of protein concentration with a Bradford protein assay kit (Bio-Rad, Hercules, CA), equal amounts of each of cytosolic and nuclear fractions were subjected to 15% SDS-PAGE, and p27<sup>KIP1</sup> was detected by immunoblot analysis as described above.

**Real-Time RT-PCR Assay.** Total RNA was isolated from H322 cells after treatment with 2  $\mu\text{M}$  erlotinib for the indicated times by phenol/chloroform extraction, and cDNA was produced with SuperScript II reverse transcription (Invitrogen, Carlsbad, CA). The standard real-time RT-PCR was performed using the following primers: p27 primer: forward, 5'-CTGCCCTCCCCAGTCTCTCT-3', and reverse, 5'-CAACGCGGGGATTCT-3'; and  $\beta$ -actin primers: forward, 5'-CATGAGCAAGCATCCTTTT-3', and reverse, 5'-CACTTCACCTCAGTTTAA-3'. Assays were performed using duplicate samples reverse transcriptase product. The p27 mRNA expression level was normalized using the  $d\text{Ct} = [\text{Ct}(\text{p27}) - \text{Ct}(\beta\text{-actin})]$  method (Livak and Schmittgen, 2001). The increase of p27 mRNA level was calculated as relative to p27 mRNA level at 0 h.

**Luciferase Activity Assay.** p27 promoter containing p27 promoter reporter construct and cDNA empty vector was a gift from Dr. T. Sakai (Department of Molecular and Cancer Pathology, Kyoto Prefectural University of Medicine, Kyoto, Japan; Inoue et al., 1999). H322 cells were transiently transfected with p27 luciferase reporter cDNA or with cDNA empty vector using a Lipofectamine kit (Invitrogen) according to the manufacturer's instructions. After transfection, cells were treated with 2  $\mu\text{M}$  erlotinib or with the same volume of medium containing 0.1% DMSO as a control for the indicated times and then harvested in 1 $\times$  lysis buffer. Luciferase activity was measured by the luciferase assay system kit (Promega). For normalization of transfection efficiency, 2  $\mu\text{g}$  of *Renilla reniformis* (sea pansy) luciferase expression plasmid (pRL-TK vector; Promega) was included in the transfection.

**p27 siRNA Transfection.** p27 siRNA and nonspecific siRNA were purchased from Dharmacon (Lafayette, CO), and transfections of p27 siRNA and nonspecific siRNA were performed with the use of Oligofectamine (Invitrogen) according to the manufacturer's instruction. After p27 siRNA transfection, cells were exposed to 2  $\mu\text{M}$  erlotinib or the same volume of medium as a control at 37°C for 24 h. Cells were washed twice with cold PBS solution, and cell pellets were

divided into two aliquots. One was for cell cycle analysis by FACS analysis as described above. The other was prepared for the determination of p27 expression by immunoblot analysis. For determination of cell growth, cells were plated on a 12-well plate and transfected with p27 siRNA or without siRNA as control. p27 siRNA-transfected and -untransfected H322 cells were exposed to 2  $\mu\text{M}$  erlotinib or to the same volume of medium as a control for the indicated times. At the specified time point, cells were harvested by trypsinization, and the viable cell numbers were assessed by trypan blue exclusion.

**Immunofluorescence Staining.** Cells were plated on a glass cover and treated with 2  $\mu\text{M}$  erlotinib or with the same volume of medium containing 0.1% DMSO as a control for 24 h. After treatment, cells were washed twice with cold PBS solution, fixed with 4% paraformaldehyde in PBS solution at room temperature for 15 min, then treated with 1% Nonidet in PBS solution for 30 min. After blocking with 5% bovine serum albumin in PBS solution for 15 min, cells were incubated with anti-p27<sup>KIP1</sup> antibody (1:500) at room temperature for 1 h. After washing three times with PBS solution, cells were incubated with fluorescence FITC-conjugated secondary antibodies (1:1000) and 100 ng/ml DAPI for 30 min in the dark room. The immunofluorescence signals were visualized with a Nikon Eclipse E400 fluorescence microscope (Nikon, Tokyo, Japan).

**Statistical Analysis.** Data are presented as mean  $\pm$  S.D. of three independent experiments. The comparisons were made with a *t* test, and the difference was considered statistically significant if the *p* value was <0.05.

## Results

**Erlotinib Induces the Inhibition of H322 Cell Growth and G<sub>1</sub>/S Phase Arrest.** First, we determined the effects of erlotinib on cell growth inhibition in medium containing 10% fetal bovine serum. Exposure to erlotinib at 0.2 to 10  $\mu\text{M}$  for 2, 4, and 12 h caused cell growth inhibition in a concentration- and time-dependent manner. The results (Fig. 1A) indicate that erlotinib at 0.2  $\mu\text{M}$  did not markedly inhibit cell growth but at 2 and 10  $\mu\text{M}$  caused approximately 30 to 43% inhibition at 24 h, 40 to 65% inhibition at 48 h, and 56 to 85% inhibition of cell growth at 72 h (*p* < 0.01). To further examine whether erlotinib could inhibit cell proliferation, we determined DNA synthesis in H322 cells after treatment with erlotinib and found that erlotinib significantly inhibited DNA synthesis in a dose-dependent manner after 24 to 48 h of treatment (data not shown). Under similar experimental conditions, inhibition of cell growth and DNA synthesis was observed in the human H358 NSCLC cell line (data not shown), indicating that the inhibition of cell growth and proliferation by erlotinib is not restricted to H322 cells.

Given the data reported previously that erlotinib causes HN5 and A431 cells to accumulate at the G<sub>1</sub> phase (Moyer et al., 1997; Pollack et al., 1999), we sought to extend these findings to H322 cells. An accumulation of cells at G<sub>1</sub> phase and reduction of S and G<sub>2</sub>/M phase cells occurred in H322 cells after treatment with different concentrations of erlotinib for 24 h or with 2  $\mu\text{M}$  erlotinib for the indicated times. Erlotinib exposures from 2 to 10  $\mu\text{M}$  resulted in a range of ~80% of cells at G<sub>1</sub> phase compared with 52% of control cells at G<sub>1</sub> phase (Fig. 1B). The time course studies demonstrate that erlotinib-induced G<sub>1</sub> phase arrest (~70% of cells) at 12 h, reached a maximum (~81%) at 24 h, and remained high over experimental periods (Fig. 1C). Furthermore, we used BrdU incorporation into DNA to determine the effect of er-



lotinib on cell-cycle progression from G<sub>1</sub> to S phase transition. As shown in Fig. 1D, the numbers of BrdU-positive cells standing for the cell cycle at S phase were dramatically reduced by ~7% after 24-h exposure to 2  $\mu$ M erlotinib compared with ~38% of BrdU-incorporated cells at time 0 and decreased to complete abolishment (~2%) after 48-h exposure. The results show that erlotinib induces cell growth inhibition accompanied by a strong blockade of cell-cycle progression from G<sub>1</sub> to S phase.

**Effects of Erlotinib on the Expression of G<sub>1</sub>/S-Related Cell Cycle Regulators, CDK Kinase Activity, and Rb Phosphorylation.** Next, we investigated the effect of erlotinib on intracellular expression of cyclins A, E, D1, D2, and CDK2 and CDK4 by immunoblot analysis. With H322 cells exposed to 2  $\mu$ M erlotinib for the indicated periods, reduction of intracellular levels of cyclin E and CDK2 oc-

curred at 12 h, and reduction of cyclin A level started at 24 h; the extents of reduction of these regulators were gradually increased thereafter. In contrast, the levels of CDK inhibitor p27<sup>KIP1</sup> were significantly induced in a time-dependent manner; i.e., the endogenous amounts of p27<sup>KIP1</sup> were barely detected at time 0 to 8 h but were clearly induced 12 h after treatment and increased thereafter. The level of p21<sup>WAF1/CIP1</sup> was barely detectable in H322 cells over time (data not shown), and the level of p130<sup>INK4a</sup> was unchanged over experiment periods (Fig. 2A). Furthermore, we found that erlotinib treatment resulted in time-dependent suppression of CDK2 activity as measured with the use of histone H1 as a substrate and reduction of CDK4 activity as assessed using p107 as a substrate (Fig. 2B). The active, phosphorylated Rb is believed to play a critical role in the regulation of cell cycle progression at the G<sub>1</sub>/S phase transition (Berthel et al.,

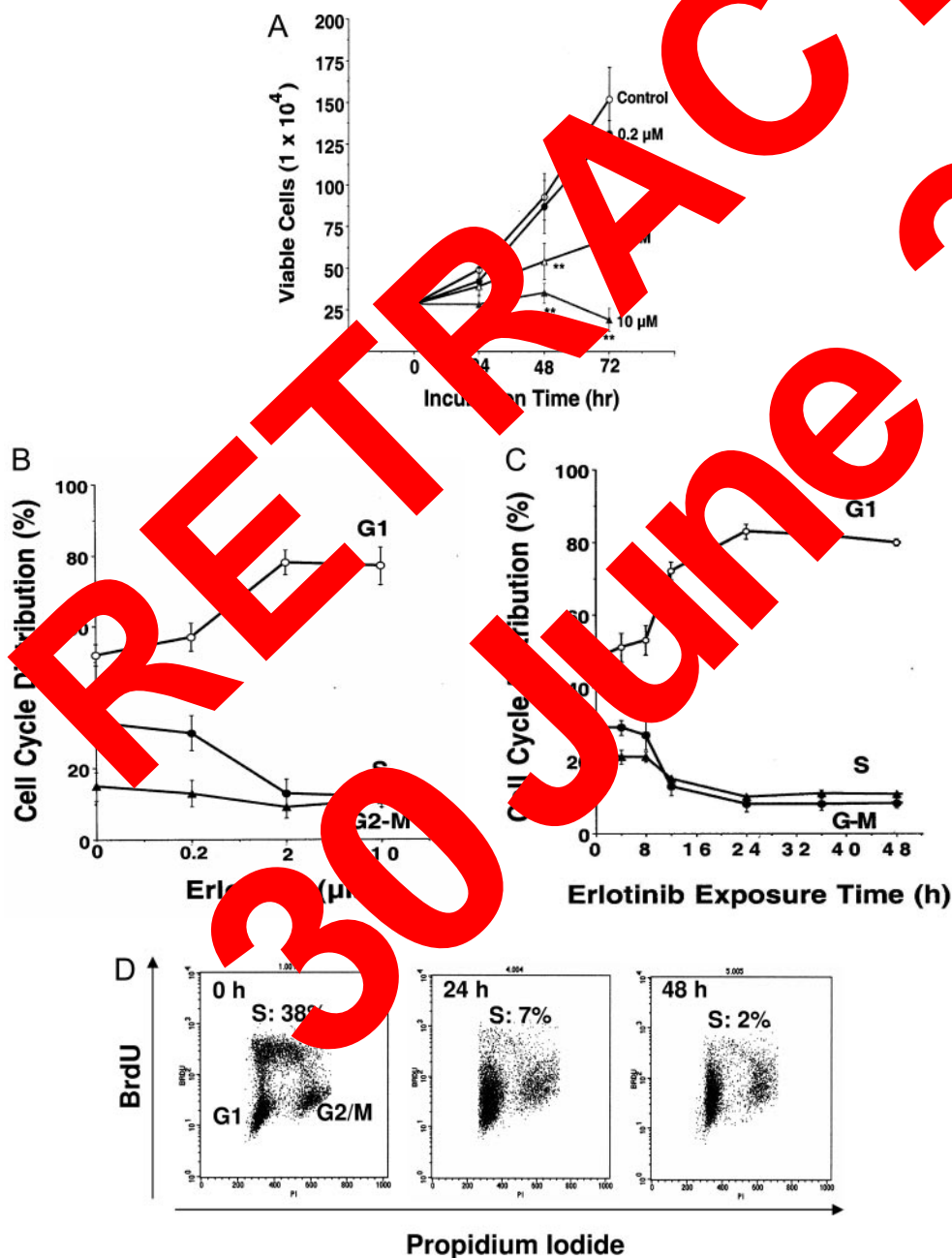


**Fig. 1.** Erlotinib induces cell growth inhibition and G<sub>1</sub>/S phase arrest in H322 cells. A, cells were incubated in the presence of 0.2, 2, and 10  $\mu$ M erlotinib or in the presence of the same volume of medium contained 0.1% DMSO as a control. At the indicated time point, viable cells were counted by trypan blue exclusion. Each point represents the mean  $\pm$  S.D. of three independent experiments. B, cells were exposed to varying concentrations of erlotinib for 24 h or to 2  $\mu$ M erlotinib (C) for the indicated time periods. After exposure, cells were stained with propidium iodide, and the cell-cycle distribution was determined by FACS analysis. Each point represents the mean  $\pm$  S.D. of three independent experiments. D, the effect of 2  $\mu$ M erlotinib on BrdU incorporation into DNA. The typical and reproducible profiles of BrdU incorporation represent a time course study of erlotinib-induced G<sub>1</sub>/S phase arrest.

2006). We therefore examined whether erlotinib-induced G<sub>1</sub> phase arrest could be involved in the disruption of Rb phosphorylation. The results shown in Fig. 2C demonstrate that erlotinib treatment led to down-regulation of total Rb protein levels and decrease in Rb protein phosphorylation as detected by slow migration of phosphorylated Rb bands in a time-dependent manner; i.e., the reduction of total Rb protein level and its phosphorylation were seen at 12 h after drug treatment and increased over experimental times. In addition, we compared the inhibitory effect of erlotinib on Rb phosphorylation at different sites probed by immunoblots using the corresponding antibodies and found that Rb phosphorylation at Ser780 and Ser795 were notably inhibited after 12 h of erlotinib exposure with similar patterns of inhibition of total Rb phosphorylation; however, p-Ser795 seemed more susceptible to erlotinib than p-Ser780. For example, Rb p-Ser795 was fully abolished but was only ~60% reduced at Rb p-Ser780 after 24 h of erlotinib exposure.

**Erlotinib Induces the Promotion of p27<sup>KIP1</sup> Gene Transcription.** To further understand the molecular mechanisms of erlotinib action on G<sub>1</sub>/S phase arrest and the in-

duction of p27<sup>KIP1</sup>, we examined the effect of erlotinib on p27<sup>KIP1</sup> expression at the protein level by immunoblots and at the transcriptional level by real-time RT-PCR analysis in H322 cells after treatment with 2 μM erlotinib for the indicated times. The results as shown in Fig. 3A demonstrate that erlotinib treatment results in the induction of p27<sup>KIP1</sup> at both protein and mRNA levels in a time-dependent manner. The time course study indicates that the elevation of p27<sup>KIP1</sup> protein amount coincides with an increase in p27<sup>KIP1</sup> mRNA levels. Real-time RT-PCR results show that erlotinib treatment results in approximately 2.8- and 6.5-fold increase in p27<sup>KIP1</sup> expression at 24 and 48 h, respectively. Next, we explored whether this effect could be caused by an activation of the p27<sup>KIP1</sup> transcriptional promoter. H322 cells were transfected with a luciferase reporter construct containing luciferase reporter controlled by promoter regions of human p27<sup>KIP1</sup> (p27 Luc, from -3568 to -549) with an empty vector as a control. As shown in Fig. 3B, erlotinib treatment led to a notable and time-dependent activation of p27<sup>KIP1</sup> promoter as measured by luciferase activity. All results suggest that the induction of p27<sup>KIP1</sup> by erlotinib may



**Fig. 2.** Erlotinib effects on cell cycle regulators, CDK activities, and Rb protein phosphorylation in H322 cells. A, exponentially growing H322 cells were treated with 2 μM erlotinib for the indicated times. After treatment, cells were harvested and prepared for the cell lysate. Equal amounts (50 μg of protein) of cell lysate were subjected to a 12% SDS-PAGE, and the protein blots were detected by immunoblots with the corresponding antibodies. β-Actin was used as a sample loading control. The quantitative analysis of expression of regulators was performed with a laser-scanning densitometer. The increased fold was expressed in comparison with the value at time 0. B, erlotinib inhibits the activities of CDK2 and CKD4. After treatment with 2 μM erlotinib for the indicated times, cells were harvested, and CDK2 and CDK4 were immunoprecipitated by the corresponding antibodies. The activity of CDK2 and CDK4 was determined by [<sup>32</sup>P]ATP incorporation into histone H1 or Rb fusion protein as described under *Materials and Methods*. The relative activity of CDK2 and CDK4 was compared with that at time 0. Each bar represents the mean ± S.D. of three independent experiments. C, erlotinib suppresses Rb phosphorylation. Cell lysates were prepared from cells followed by exposure to 2 μM erlotinib for the indicated times, and total Rb and p-Rb at Ser780 or Ser795 were detected by immunoblots with the corresponding antibodies. β-Actin was used as a sample loading control. The quantitative analysis of each band was performed with a laser-scanning densitometer. The increased folds were calculated in comparison with the value at time 0.

be due, at least in part, to the activation of p27<sup>KIP1</sup> at the transcriptional level.

**Erlotinib Induces p27<sup>KIP1</sup> Protein Stabilization.** Aside from induction of p27<sup>KIP1</sup> transcription, the increase in the intracellular amount of p27<sup>KIP1</sup> could be caused by a reduction of p27<sup>KIP1</sup> protein degradation via suppression of its phosphorylation at Thr187 or interaction with the SKP2-mediated ubiquitin/proteasome pathway (Tsvetkov et al., 1999). To test this possibility, we examined p27<sup>KIP1</sup> phosphorylation at Thr187 and the expression of SKP2 in H322 cells after treatment with 2  $\mu$ M erlotinib for the indicated times. The results shown in Fig. 4A demonstrate that erlotinib treatment caused a time-dependent reduction of p27<sup>KIP1</sup> phosphorylation at Thr187 and decrease in SKP2 expression. It is interesting that the time point at which the reduction of p27<sup>KIP1</sup> p-Thr187 and SKP2 occurred (12 h after erlotinib treatment) was tightly consistent with the accumulation of p27<sup>KIP1</sup>. To further test the hypothesis that the increased level of p27<sup>KIP1</sup> protein in erlotinib-treated cells is caused by stabilization of p27<sup>KIP1</sup> protein, we determined the effect of erlotinib on p27<sup>KIP1</sup> stability in a pulse-chase experiment. The results as shown in Fig. 4B indicate that p27<sup>KIP1</sup> protein was rapidly degraded with calculated half-life time ( $t_{1/2}$ ) of  $\sim$ 1.8 h in control cells, whereas the p27<sup>KIP1</sup> protein was stable with  $t_{1/2}$  of  $\sim$ 6 h in erlotinib-treated cells. The accumulation of p27<sup>KIP1</sup> protein in cells treated with erlotinib may be caused by the activation of p27<sup>KIP1</sup> transcriptional level and/or increase in p27<sup>KIP1</sup> stability.

**Erlotinib Induces Nuclear Localization of p27<sup>KIP1</sup> Protein.** Recent reports suggest that erlotinib-induced G<sub>1</sub> phase arrest and suppression of cell growth was associated with subcellular localization of p27<sup>KIP1</sup> from cytoplasm to nucleus (Liang et al., 2002). Here, we sought to determine whether erlotinib-induced cell G<sub>1</sub> arrest could be involved in the alteration of p27<sup>KIP1</sup> subcellular localization. First, we performed immunofluorescence staining experiments to observe the localization of p27<sup>KIP1</sup> in H322 cells after 24 h of exposure to 2  $\mu$ M erlotinib or with the same volume of

medium contained 0.1% DMSO as a control. Figure 5A shows a representative example of immunofluorescence staining, which shows that erlotinib treatment leads to p27<sup>KIP1</sup> localization in the nucleus ( $48 \pm 10\%$  of cells) compared with that in control cells (only  $9 \pm 7\%$  of cells). To determine the levels of p27<sup>KIP1</sup> in cytosolic and nuclear fractions by immunoblot analysis, we consistently found that p27<sup>KIP1</sup> was detected predominantly in the nuclear fraction and to a lesser extent in cytosolic fraction in erlotinib-treated cells, whereas low levels of p27<sup>KIP1</sup> protein were detected in both cytosolic and nuclear fractions of untreated cells (Fig. 5B). These results suggest that the accumulation of p27<sup>KIP1</sup> protein in the nucleus may be an event in the response to erlotinib-induced G<sub>1</sub>/S phase arrest and cell growth inhibition.

**Effect of Knockdown of p27<sup>KIP1</sup> Expression by p27<sup>KIP1</sup> siRNA on Erlotinib-Induced G<sub>1</sub> Phase Arrest and Cell Growth Inhibition.** Next, we explored whether p27<sup>KIP1</sup> accumulation could directly cause the blockade of G<sub>1</sub> phase and cell growth inhibition in response to erlotinib stress. For this purpose, we used p27 siRNA to down-regulate p27<sup>KIP1</sup> expression. As shown in Fig. 6A, immunoblot analysis indicated that p27 siRNA effectively and specifically led to the knockdown of p27<sup>KIP1</sup> protein expression in both erlotinib-treated and control cells; transfection with nonspecific siRNA did not significantly affect erlotinib-induced accumulation of p27<sup>KIP1</sup> compared with that in p27<sup>KIP1</sup> changes in untransfected cells. We then determined whether the accumulation of p27<sup>KIP1</sup> is required in response to erlotinib-induced G<sub>1</sub> arrest and growth inhibition. The results from the analysis of cell cycle distribution by FACS flow cytometry showed that the down-regulation of p27<sup>KIP1</sup> by siRNA results in a partial decrease in erlotinib-induced G<sub>1</sub> arrest (60% of G<sub>1</sub> cells) relative to approximately 78 and 72% cells at G<sub>1</sub> in untransfected and nonspecific siRNA-transfected cells, respectively, after erlotinib treatment with erlotinib (Fig. 6B). Cell growth assessment also demonstrated that down-regulation of p27<sup>KIP1</sup> ex-

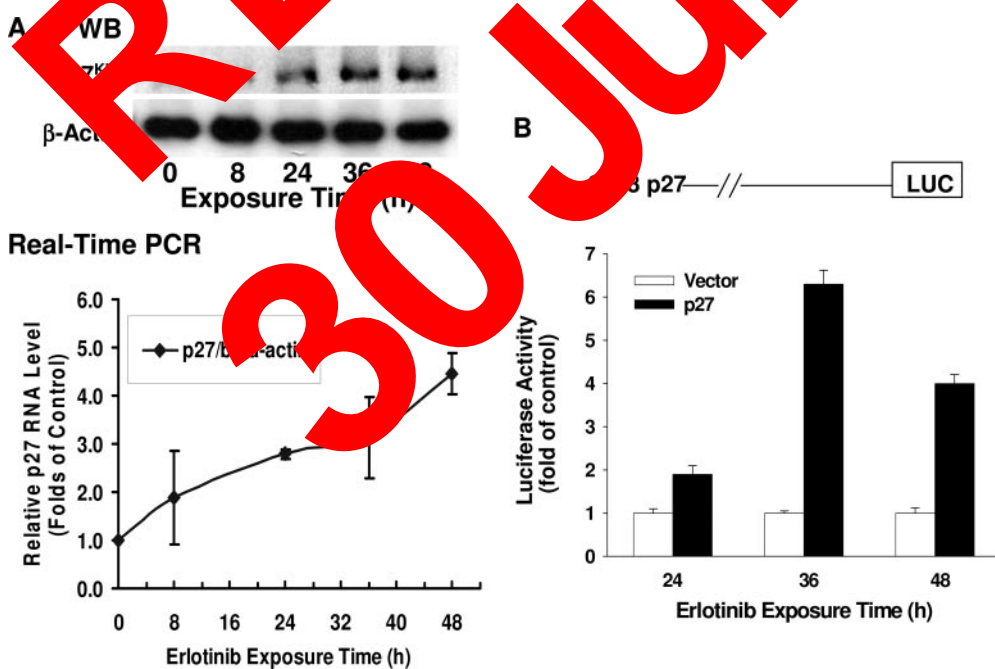


**Fig. 3.** Erlotinib induces the promotion of p27<sup>KIP1</sup> gene expression in H322 cells. A, cells were exposed to 2  $\mu$ M erlotinib for the indicated times. After exposure, cells were harvested and divided into two aliquots. One was for the determination of the amount of p27<sup>KIP1</sup> protein by immunoblots.  $\beta$ -Actin was used as a sample loading control. The other aliquot was for extraction of total RNA to determine p27<sup>KIP1</sup> mRNA level by using real-time PCR. Each point represents the mean  $\pm$  S.D. of three independent experiments. B, H322 cells were transiently transfected with p27 luciferase reporter construct or with cDNA empty plasmid vector. After a 6-h transfection, cells were washed and incubated in the fresh medium containing 2  $\mu$ M erlotinib for the indicated times. Luciferase activity was determined with a luciferase assay system kit. Each bar represents the mean  $\pm$  S.D. of two independent experiments.



pression by p27 siRNA resulted in a significant reduction of erlotinib-induced cell growth inhibition over experimental periods (Fig. 6C). The data suggest that the increase in p27<sup>KIP1</sup> expression by erlotinib contributes to cell cycle arrest at G<sub>1</sub> and cell growth inhibition.

**Relationship between G<sub>1</sub> Phase Arrest and Cell Sensitivity to Erlotinib.** G<sub>1</sub>/S phase arrest may be a major contributor to erlotinib-induced cell growth inhibition in H322 cells. Thus, we needed to determine whether there was a relationship between cell cycle response and cell sensitivity to erlotinib. We chose two sensitive NSCLC cell lines (H322, H358), human skin epidermoid carcinoma A431 cells, and human head and neck carcinoma HN5 cells, which are known to be sensitive to erlotinib (Moyer et al., 1997; Pollack et al., 1999), and four resistant NSCLC cell lines (H460, A549, H596, and H1299 cells) as models and exposed them to erlotinib at 2  $\mu$ M, a concentration that is close to clinically effective doses (Hidalgo et al., 2001). After 72 h of exposure, cell survival was assessed by MTT assay. The results shown in Fig. 7, A and B, indicate that 2  $\mu$ M erlotinib causes >50% cell growth inhibition ( $P < 0.01$ ) in all tested sensitive cell lines but had less effect in all tested resistant cell lines. A 24-h exposure to 2  $\mu$ M erlotinib consistently resulted in a significant increase in G<sub>1</sub> phase cell accumulation in sensitive cell lines tested, but lesser extents of G<sub>1</sub> cell accumulation was observed in resistant cell lines (Fig. 7, C and D). Moreover, immunoblot analysis revealed that whereas erlotinib treatment led to suppression of p27<sup>KIP1</sup> decrease in cyclin A expression, and induction of p27<sup>KIP1</sup> in all tested sensitive cells, no noticeable effect was observed in resistant cell lines (Fig. 7, E and F). These results suggest that G<sub>1</sub>/S phase arrest, the up-regulation of p27<sup>KIP1</sup>, and the alteration in the expression of cell cycle regulators may be at least partly associated with NSCLC cell response to erlotinib.

## Discussion

In a previous work, we demonstrated that erlotinib as a highly selective EGFR tyrosine kinase inhibitor induced suppression of serum- or EGF-activated EGFR activity and its mediated downstream pathways. It also inhibits the activation of PKB/AKT, Ras/Raf/MEK/extracellular signal-regulated kinase, and Stat family in several human NSCLC cell lines (Adjei, 2006). In this work, we demonstrated that erlotinib strongly inhibits H322 cell growth and proliferation and blocks cell cycle progression at G<sub>1</sub>/S phase transition. To better understand the molecular mechanisms underlying erlotinib-induced cell growth inhibition and cell cycle arrest, we determined the effect of erlotinib on the expression of key regulatory proteins that are required for transition from G<sub>1</sub>/S phase restriction point of cell cycle progression. Indeed, we found that erlotinib induced a time-dependent decrease in cyclin D1 and cyclin E expression and inhibition of CDK2 activity. Several reports have demonstrated that G<sub>1</sub>-phase arrest induced by inhibition of mitogen-activated signaling pathways is accompanied by down-regulation of D-type cyclins as a primary suppression of CDK4 activity (Baldin et al., 1996). In our work, we found that erlotinib treatment significantly suppressed CDK2 activity, but did not markedly affect the levels of cyclin D1 and cyclin E in H322 cells. To certify our conclusions, we used two different epitope-mapping anti-cyclin D1 antibodies to determine cyclin D1 levels in lysates from erlotinib treatment and control cells, and similar results, indicating that the results should be believable. In addition, our preliminary results showed that erlotinib induced G<sub>1</sub> phase arrest but did not markedly change cyclin D1 expression in H358 cells (data not shown). The reasons for cyclin D level being stable in erlotinib-induced G<sub>1</sub> cells remain to be understood. One possibility may be that H322 cells have too high levels of cyclin D1 to change its levels after erlotinib

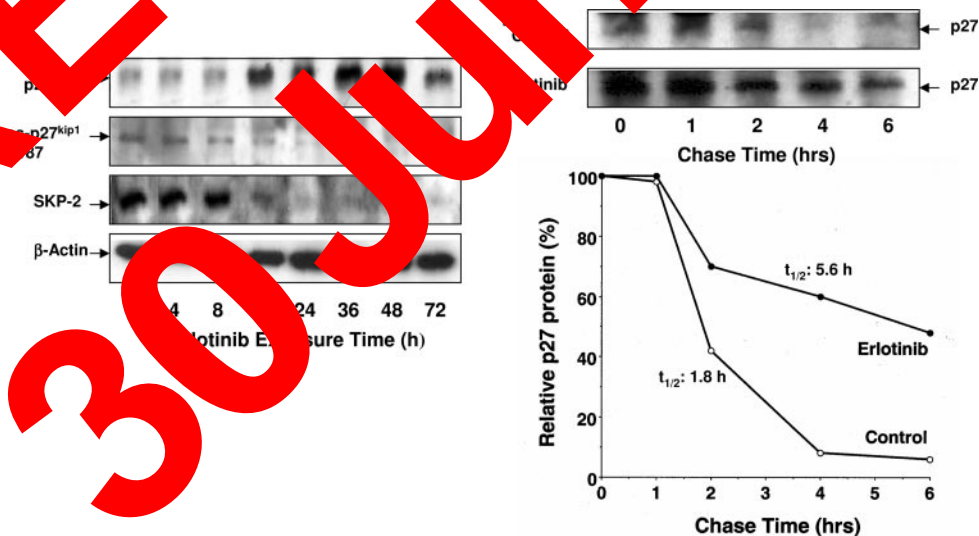


**Fig. 4.** Erlotinib-induced p27<sup>KIP1</sup> accumulation and stabilization mediated by the inhibition of phosphorylation of p27<sup>KIP1</sup> at Thr187 and the level of SKP-2 protein. A, H322 cells were exposed to 2  $\mu$ M erlotinib for the indicated times. After exposure, the levels of p27<sup>KIP1</sup>, p-p27<sup>KIP1</sup> Thr187, and SKP-2 were detected by immunoblots with the corresponding antibodies.  $\beta$ -Actin was used as a sample loading control. B, effect of erlotinib on p27<sup>KIP1</sup> stabilization. H322 cells were exposed to 2  $\mu$ M erlotinib or to the same volume of medium containing 0.1% DMSO as a control. After 24-h exposure, cells were washed three times with medium and then reincubated in the fresh medium containing 50  $\mu$ g/ml cycloheximide. After incubation at the indicated time period, cells were taken from culture for the determination of the level of p27<sup>KIP1</sup> as detected by immunoblots with anti-p27<sup>KIP1</sup> antibody. The quantitative analysis of p27<sup>KIP1</sup> in each time point was performed with a laser-scanning densitometer. The relative p27<sup>KIP1</sup> level was expressed compared with the level of p27<sup>KIP1</sup> at chase time 0.

treatment. In addition, we suggest that erlotinib-induced suppression of CDK4 activity may be mediated via unidentified factors that could be required for the activation of CDK4. Recent reports have demonstrated that inhibition of cyclin A/CDK2 or cyclin E/CDK2 is implicated in the suppression of CDK4 activity (Koff et al., 1992). In this work, we demonstrated that erlotinib treatment causes a time-dependent decrease in the levels of total Rb protein and inhibition of Rb phosphorylation. In addition, erlotinib inhibits Rb phosphorylation at different serine residues, particularly at Ser795, which was more susceptible than that at Ser780, suggesting that erlotinib could act on Rb phosphorylation at specific sites, by which it may specifically affect Rb protein binding to a particular partner. In addition, recent reports have shown that the ERK1/2 pathway may be involved in EGF-induced rapid Rb protein phosphorylation at Ser780 and Ser795 (Guo et al., 2005). We examined whether erlotinib-induced inhibition of Rb phosphorylation at Ser795 or Ser780 could be associated with inhibition of ERK1/2 and/or PI3/AKT related pathways. Our preliminary data show that only erlotinib and U0126, an ERK1/2 inhibitor, but not LY294002, a PI3/AKT inhibitor, caused the suppression of Rb phosphorylation at Ser795 and Ser780, suggesting that erlotinib-induced phosphorylation

may be at least in part associated with the inhibition of ERK1/2-related pathways (data not shown).

It has been well-established that cyclin-CDK inhibitors CIP/KIP p21, p27, and INK4 p15, p16, and p18 as the negative controllers play important roles in the regulation of cell cycle progression. Recent studies have shown that p21<sup>WAF1/CIP1</sup> and p27<sup>KIP1</sup> are necessary for the assembly of the cyclin A/CDK4 or CDK6 and the formation of cyclin A/CDK2 or cyclin E/CDK2 complexes. Thus, an increase in the expression of p21<sup>WAF1/CIP1</sup> and p27<sup>KIP1</sup> would facilitate assembly of the complexes and result in suppression of the activity of cyclin/CDK complexes, thereby delay cell cycle progression (Slings and Pagano, 2000). In this work, we determined the effect of erlotinib on the expression of CIP/KIP inhibitors. We found that erlotinib did not affect the expression of p15<sup>INK4a</sup> over experiment times. The endogenous levels of p21<sup>WAF1/CIP1</sup> in H322 cells were barely detectable, and erlotinib did not induce p21<sup>WAF1/CIP1</sup> expression. However, we found that p27<sup>KIP1</sup> levels were markedly increased by erlotinib in a time-dependent manner. The increase in p27<sup>KIP1</sup> levels is highly correlated with cell cycle arrest. It has been known that expression of p27<sup>KIP1</sup> is regulated at transcriptional and post-transcriptional

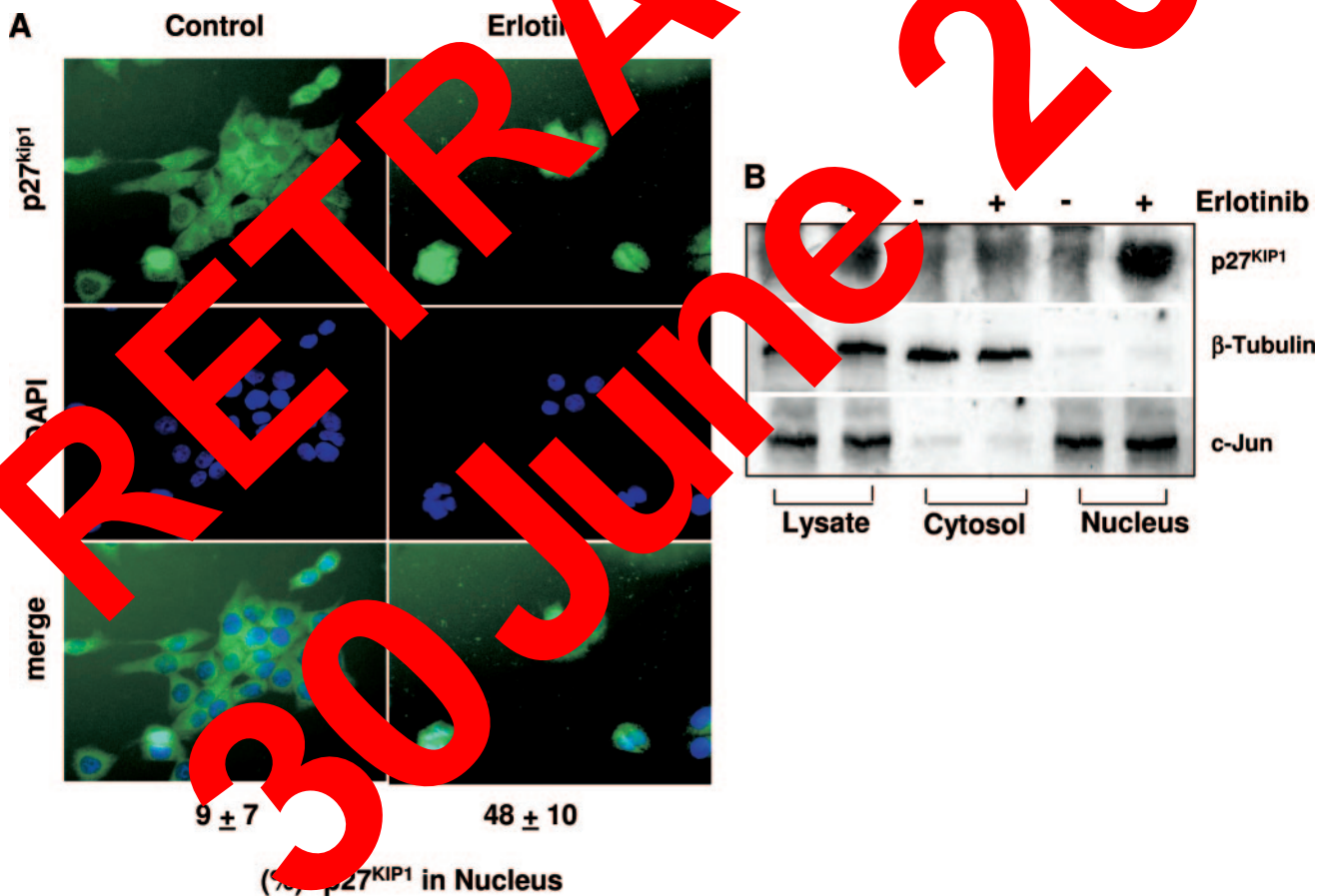


**Fig. 5.** Erlotinib induces p27<sup>KIP1</sup> localization to the nucleus. **A**, H322 cells were plated on a glass cover overnight and then exposed to 2  $\mu$ M erlotinib or to the same volume of medium containing 0.1% DMSO as a control. After 24 h of exposure, cells were fixed with 4% paraformaldehyde for 15 min and permeabilization with 1% Nonidet P-40 for 30 min. After incubation with monoclonal anti-p27<sup>KIP1</sup> antibodies at room temperature for 1 h, cells were incubated with FITC-conjugated secondary antibody and 100 ng/ml DAPI solution for 30 min in a dark room. The p27<sup>KIP1</sup> localization and DAPI-stained nucleus were visualized with a Nikon Eclipse E400 fluorescence microscope. The percentage of cells with a p27<sup>KIP1</sup>-stained nucleus represents the mean  $\pm$  S.D. of three independent experiments of counting at least 200 cells. **B**, after 24 h of exposure to 2  $\mu$ M erlotinib or the same of volume of medium containing 0.1% DMSO as a control, the extractions of total cell lysates, cytosolic, and nuclear fractions were performed as described under *Materials and Methods*. The levels of p27<sup>KIP1</sup> were detected by immunoblots with monoclonal anti-p27<sup>KIP1</sup> antibody.  $\beta$ -Tubulin was used as a cytosolic fraction loading control and c-Jun as a nuclear fraction loading control, respectively.



tional levels in different types of cells (Besson et al., 2006). We found that the erlotinib-induced increase in p27<sup>KIP1</sup> level was mediated through up-regulation of gene transcriptional activity and via inhibition of protein degradation. The results from quantitative real-time RT-PCR showed that an increase in p27 mRNA expression was tightly correlation with an increase in p27<sup>KIP1</sup> protein in cells treated with erlotinib. We also provide evidence that the region from -3568 to -549 of the p27<sup>KIP1</sup> promoter plays an important role in erlotinib-induced p27<sup>KIP1</sup> gene transcription. Several reports have shown that the transcriptional regulation of p27<sup>KIP1</sup> promoter activity seems to be complex and consists of both positive and negative regulatory elements. Multiple transcriptional factor binding sites within the p27<sup>KIP1</sup> promoter have been characterized, including forkhead transcription factor (Dijkers et al., 2000), SP1 (Fischer et al., 2005), and E2F (Wang et al., 2005). Although our results showed that erlotinib caused the up-regulation of p27<sup>KIP1</sup> expression, the mechanism by which erlotinib-induced promotion of p27<sup>KIP1</sup> gene transcription remains to be further elucidated. Besides activation of gene expression, the increase in p27<sup>KIP1</sup> level may

depend on the post-translational regulation by the prevention of proteolytic degradation. Several studies have demonstrated that the ubiquitin-proteasome proteolysis system is a major pathway for the regulation of p27<sup>KIP1</sup> levels (Boehm et al., 2002). It has been shown that phosphorylation of p27<sup>KIP1</sup> at Thr187 by CDK2 appeared p27<sup>KIP1</sup> protein for binding to ubiquitin ligase E3-SCF-SKP2 that leads to 26S proteasome degradation (Morignoli et al., 1999). In our study, erlotinib treatment consistently resulted in a time-dependent reduction of p27<sup>KIP1</sup> phosphorylation at Thr187 and decrease in SKP2 levels. Overall, our findings suggest that G<sub>1</sub>/S phase arrest by erlotinib was at least in part mediated through the accumulation of p27<sup>KIP1</sup>, which was regulated by the promotion of gene expression and decrease of protein degradation. Recent studies have shown that localization of p27<sup>KIP1</sup> protein in the nucleus is required to inhibit CDK activation by CDK-activating kinase (Kobayashi et al., 1999). In addition, p27<sup>KIP1</sup> localization is essential for controlling the cell cycle progression and cell proliferation (Jiang et al., 2000). In this work we have investigated the effect of erlotinib on p27<sup>KIP1</sup> subcellular localization and found that the p27<sup>KIP1</sup>

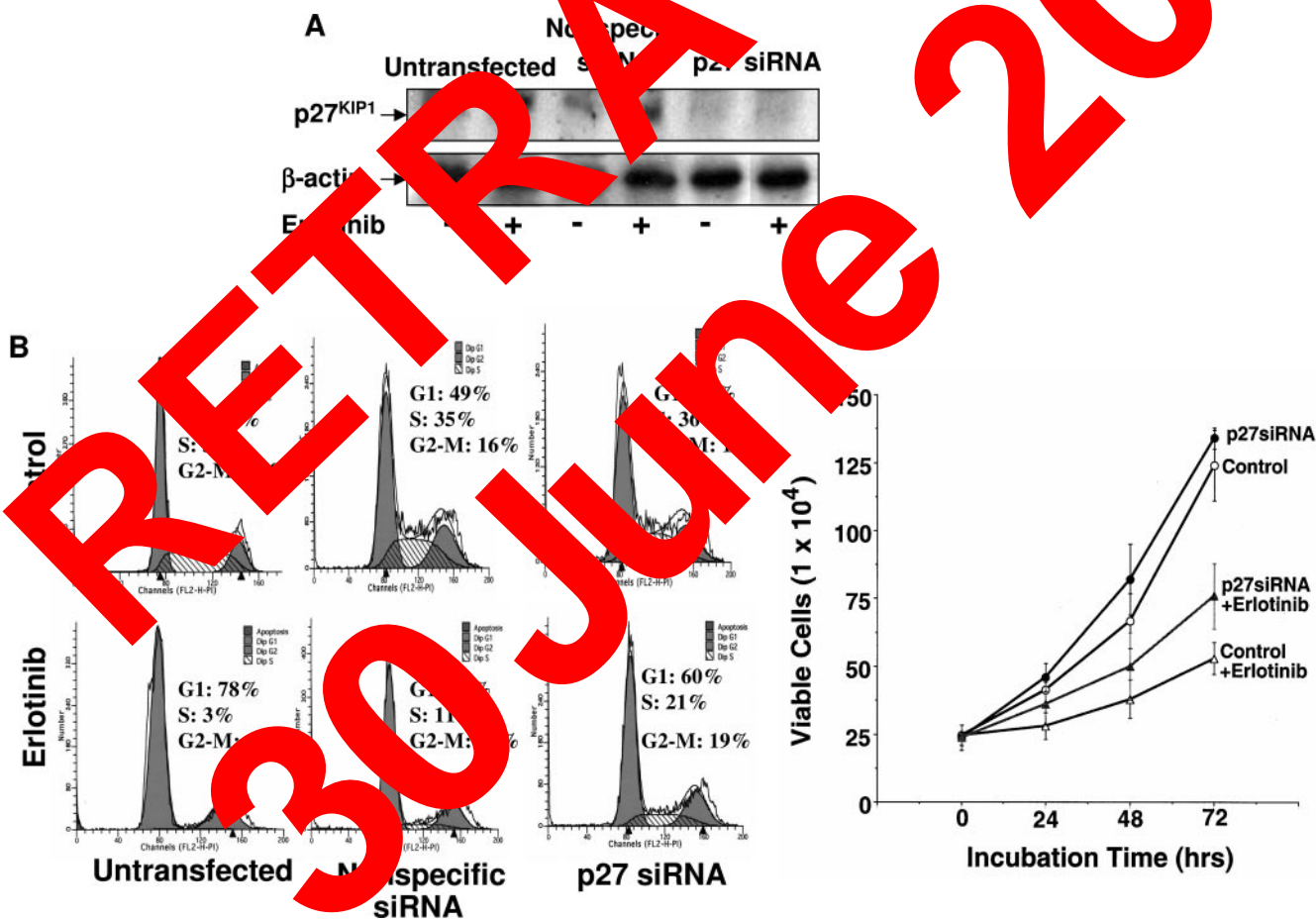


**Fig. 6.** Knockdown of p27<sup>KIP1</sup> expression by p27<sup>KIP1</sup> siRNA attenuates erlotinib-induced G<sub>1</sub> arrest and cell growth inhibition of H322 cells. After transfection with p27<sup>KIP1</sup> siRNA or with nonspecific siRNA and with the same volume of medium as an untransfection, cells were incubated in the presence of 2  $\mu$ M erlotinib or the same of medium containing 0.1% DMSO as a control. After 24 h of incubation, cells were taken from culture and divided into two aliquots. One was for the determination of p27<sup>KIP1</sup> expression by immunoblots with anti-p27<sup>KIP1</sup> antibody.  $\beta$ -Actin was used as a loading control (A). The other aliquot was for determination of cell cycle distribution by FACS analysis after cell staining with propidium iodide (B). For determination of cell growth, H322 cells were plated on a 24-well plate and transfected with p27<sup>KIP1</sup> siRNA or with the same volume of medium as a control. After transfection, cells were incubated in the medium in the presence of 2  $\mu$ M erlotinib or the same volume of medium containing 0.1% DMSO as a control at 37°C for the indicated times. At the time point, cells were harvested, and viable cells were assessed by trypan blue exclusion. Each point represents the mean  $\pm$  S.D. of three independent experiments (C). \*,  $P < 0.05$ .

protein was significantly accumulated in the nucleus in erlotinib-treated cells compared with its predominant localization in the cytoplasm in control cells, suggesting that the alteration of p27<sup>KIP1</sup> localization may be involved in the cell cycle arrest at G<sub>1</sub>/S phase and inhibition of cell proliferation. Several reports have shown that phosphorylation of p27<sup>KIP1</sup> is an important determinant of its subcellular localization. It has been evident that phosphorylation of p27<sup>KIP1</sup> at Thr157 mediated by PKB/AKT results in retention of p27<sup>KIP1</sup> in the cytoplasm and prevention of G<sub>1</sub> arrest (Shin et al., 2002). Ser10 is another phosphorylation site of p27<sup>KIP1</sup> for the nuclear export of the protein mediated by exportin (Viglietto et al., 2002). Recent studies have consistently showed that the inhibition of p27<sup>KIP1</sup> phosphorylation at Thr157 by LY294002 causes p27<sup>KIP1</sup> accumulation in the nucleus and cell growth inhibition (Shin et al., 2005). In addition, it has been reported that inhibition of cyclin E/CDK2 results in the retention of p27<sup>KIP1</sup> in nucleus (Ishida et al., 2002). Therefore, we

suggest that erlotinib-induced p27<sup>KIP1</sup> accumulation in the nucleus may be caused by the suppression of activity of the EGFR-PKB/AKT axis and/or by the reduction of cyclin E/CDK2 as described above. It is interesting that knock-down of p27<sup>KIP1</sup> expression by siRNA resulted in the attenuation of G<sub>1</sub> phase arrest and growth inhibition, indicating that the induction of p27<sup>KIP1</sup> is essential for erlotinib-induced G<sub>1</sub> arrest and cell growth inhibition. These results are consistent with studies by Le et al. (2006), who showed that reduction of p27<sup>KIP1</sup> using p27<sup>KIP1</sup> siRNA blocked anti-HER2 antibody-induced p27<sup>KIP1</sup> up-regulation and G<sub>1</sub> arrest in breast cancer cells. Finally, our results demonstrate a direct relationship between G<sub>1</sub> phase and cell sensitivity to erlotinib. These results are consistent with other reports, which showed that inhibition of ErbB-2 pathways by AG1478 caused G<sub>1</sub> phase arrest with accumulation of p27<sup>KIP1</sup> and a decrease in the cyclin E/CDK2 complex in the human breast MCF-7/ErbB2-overexpressing cell line (Sferink et



**Fig. 7.** Relationship between G<sub>1</sub>/S arrest and cell sensitivity to erlotinib in human NSCLC cell lines. Erlotinib-sensitive cell lines (H322, H358, A431, and HN5) and erlotinib-resistant cell lines (H460, A549, H596, and H1299) were seeded on a 96-well plate and exposed to 2  $\mu$ M erlotinib or to the same volume of medium containing 0.1% DMSO as a control for 72 h. After exposure, the cell survival in sensitive (A) and resistant cell lines (B) was assessed by MTT assay. The percentage of cell survival in erlotinib-treated cells was calculated in comparison with the value of control as 100%. Each bar represents the mean  $\pm$  S.D. of three independent experiments. \*\*,  $P < 0.01$ . For the determination of G<sub>1</sub> phase arrest by erlotinib, the tested sensitive (C) and resistant cell lines (D) were seeded on a six-well plate and exposed to 2  $\mu$ M erlotinib or to the same volume of medium containing 0.1% DMSO as a control. After 24 h of exposure, cells were harvested and divided into two aliquots. One was for the assay of cell cycle distribution by FACS analysis after cell staining with propidium iodide. Each bar represents the mean  $\pm$  S.D. of three independent experiments. \*\*,  $p < 0.01$ . The other cell aliquots were for the preparation of cell lysates to determine levels of p-Rb, cyclin A, and p27<sup>KIP1</sup> by immunoblot analysis.  $\beta$ -Actin was used as a sample loading control. The quantitative analysis of p-Rb, cyclin A, and p27<sup>KIP1</sup> in sensitive (E) and resistant cell lines (F) was performed with a laser-scanning densitometer. The increased fold in erlotinib-treated cells was calculated in comparison with the value of control as 1.

al., 2001). Nahta et al. (2004) showed that down-regulation of p27<sup>KIP1</sup> in breast cancer cell lines was associated with both an increase in cell cycle S-phase fraction and with cell resistance to trastuzumab, an anti-erbB-2/Neu monoclonal antibody. We found consistently that induction of p27<sup>KIP1</sup> was necessary in response to erlotinib-induced cell growth inhibition and G<sub>1</sub>/S arrest, suggesting the induction and accumulation of p27<sup>KIP1</sup> may be one of the important determinants in response to erlotinib-induced cell cycle blockade and cell growth inhibition.

#### Acknowledgments

We thank Ruoping Lin for technical support.

#### References

- Adjei AA (2006) Novel combinations based on epidermal growth inhibition. *Clin Cancer Res* **12**:4446s–4450s.
- Baldin V, Lukas J, Marcote MJ, Pagano M, and Draetta G (1993) Cyclin D1 is a nuclear protein required for cell cycle progression in G1. *Genes Dev* **7**:812–821.
- Berthet C, Klarmann KD, Hilton M, Suh HC, Keller JR, Kiyokawa H, and Kaldis P (2006) Combined loss of cdk2 and cdk4 results in embryonic lethality and Rb hypophosphorylation. *Dev Cell* **10**:563–573.
- Besson A, Gurian-West M, Chen X, Kelly-Spratt KS, Kemp CJ, and Roberts JM (2006) A pathway in quiescent cells that controls p27<sup>KIP1</sup> stability, subcellular localization, and tumor suppression. *Genes Dev* **20**:47–64.
- Boehm M, Yoshimoto T, Crook MF, Nallamshetty S, True A, Nobel GJ, and Nobel EG (2002) A growth factor-dependent nuclear kinase phosphorylates p27 and regulates cell cycle progression. *EMBO J* **21**:3390–3401.
- Chellappan SS, Giordano A, and Fisher PB (1998) Role of cyclin dependent kinases and their inhibitors in cellular differentiation and development. *Curr Top Microbiol Immunol* **227**:57–103.
- Dijkers PF, Medma RH, Pals C, Banerji L, Thomas N, van der W, Burger WM, Raaijmakers JA, Lammers JW, Koenderman L, et al. (2006) *Mol Cell Biol* **26**:9138–9148.
- Dyson N (1998) The regulation of E2F by pRB-family proteins. *Genes Dev* **12**:2245–2262.
- Fischer C, Sanchez-Ruderish H, Welzei M, Gienemann M, Nakai T, Anagnostou G, Gabius H-J, Khachigian L, Detjen KM, and Stetler-Stevenson S (2006) Selectin-1 interacts with the  $\alpha 5 \beta 1$  fibronectin receptor to regulate carcinoma cell growth via induction of p21 and p27. *J Biol Chem* **280**:37260–37267.
- Guo J, Sheng G, and Warner RL (2006) Epidermal growth factor-induced rapid retinoblastoma phosphorylation at Ser780 and Ser795 is mediated by ERK1/2 in small intestine epithelial cells. *J Biol Chem* **281**:35992–35998.
- Haeder M, Rotsch M, Bock G, Havemann K, Hentschel B, and Moelling K (1988) Epidermal growth factor receptor expression in human lung cancer cell lines. *Cancer Res* **48**:1136–1136.
- Herbst RS and Bunz M (2004) Targeting the epidermal growth factor receptor in non-small cell lung cancer. *Clin Cancer Res* **9**:5813–5824.
- Hidalgo M, Siu LL, and Sznol L (2001) Phase I and pharmacology studies with OSI-777, an epidermal growth factor receptor tyrosine kinase inhibitor in patients with advanced solid malignancies. *Clin Oncol* **19**:3267–3279.
- Inoue M, Kamiya T, and Sakai A (1999) Sp1 and NF-Y synergistically mediate the effect of vitamin D3 in the p27<sup>KIP1</sup> gene promoter. *Oncogene* **19**:32309–32317.
- Ishida M, Nakai T, Kamei T, Yoshida M, Nakayama K, and Nakayama K (2001) Phosphorylation of p27<sup>KIP1</sup> on serine 10 is required for its binding to MDM2 nuclear export. *J Biol Chem* **277**:14355–14358.
- Jiang Y, Zhang Y, and Vertaille CM (2000) Abnormal integrin-mediated regulation of chronic myelogenous leukemia CD34<sup>+</sup> cell proliferation: RCB/ABL up-regulates the cyclin-dependent kinase inhibitor, p27<sup>KIP1</sup>, which is relocated to the cell cytoplasm and incapable of regulating p32 activity. *Proc Natl Acad Sci U S A* **97**:10538–10543.
- Klapper LN, Kirschbaum MH, Sela M, and Golden Y (2006) Biochemical and clinical implications of the ErbB/HER signaling network of growth factor receptors. *Adv Cancer Res* **77**:25–79.
- Koff A, Giordano A, Desai S, Ramakrishna K, Lee J, Weng J, Edge S, Nishimoto T, Morgan DO, Franza BR, and Roberts JM (1995) Identification and activation of a cyclin E-cdk2 complex during the G1/S transition of the human cell cycle. *Science* **257**:1689–1694.
- Le X-F, Claret FX, Lammayot A, Ting L, Deshpande D, LaPushin R, Tar AM, and Bast RC Jr (2003) The role of cyclin-dependent kinase inhibitor p27<sup>KIP1</sup> is anti-HER2 antibody-induced G1 cell cycle arrest and tumor growth inhibition. *J Biol Chem* **278**:23441–23450.
- Lenferink AEG, Busse D, Flanagan M, Yakes FM, and Arteaga L (2001) ErbB2/neu kinase modulates cellular p27<sup>KIP1</sup> and cyclin D1 through multiple signaling pathways. *Cancer Res* **61**:6583–6591.
- Liang J, Zubovitz J, Petrocelli T, Kotchetkov R, Lee J, Lee K, Lee JH, Ciarallo S, Catzavelovlos C, Beniston R, et al. (2005) PKB/Akt phosphorylates p27, impairs nuclear import of p27 and opposes p27-mediated G1 arrest. *Nat Med* **8**:1153–1160.
- Livak KJ and Schmittgen TD (2001) Analysis of relative gene expression data using real-time quantitative PCR and 2<sup>- $\Delta\Delta$ CT</sup> method. *Methods* **25**:402–408.
- Matsushime H, Rousset MF, Akiyama RA, and Sherr CJ (1991) Colony-stimulating factor 1 regulated nuclear cyclin during G1 phase of cell cycle. *Cell* **65**:701–713.
- Montagnoli A, Fiore F, Eyraud-Cassier AC, Draetta GF, Hershko A, and Pagano M (1999) Ubiquitination of p27<sup>KIP1</sup> mediated by cyclin-dependent phosphatase and trimeric complex formation. *Cell Dev* **13**:1181–1189.
- Moyer JD, Barlow DG, Iwata K, Goldstein B, Cunningham DD, and Doty J (2005) Moyer MP, et al. Induction of apoptosis by p27<sup>KIP1</sup> overexpression and arrest by p27<sup>KIP1</sup> inhibitor of epidermal growth factor tyrosine kinase. *Cancer Res* **57**:4463–4468.
- Nahta R, Takahashi T, Hung M-C, and Esteva I (2004) p27<sup>KIP1</sup> down-regulation is associated with trastuzumab resistance in breast cancer cells. *Cancer Res* **64**:3981–3986.
- Nonberg SB and Benz CC (2000) Tyrosine kinase inhibitors bind to the epidermal growth factor receptor subfamily: role as anticancer agents. *Cancer Res* **59**:753–767.
- Palack VA, Savar DM, Baker DA, Tsapras A, Pustilnik DE, Moyer J, and Barbacci P (2006) Inhibition of epidermal growth factor receptor-associated tyrosine phosphorylation in human carcinoma with gefitinib: dynamics of receptor inhibition in situ and antitumor effects in athymic mice. *J Pharmacol Exp Ther* **297**:748–758.
- Pfeiffer D, Brandt R, Ciardiello T, and Nishino N (1998) Epidermal growth factor-related peptides and their receptors in human malignancies. *Crit Rev Oncol Hematol* **19**:183–232.
- Scagliotti GV, Selvaggi G, Tjuland S, and Hirsch FR (2004) The biology of epidermal growth factor receptor in lung cancer. *Clin Cancer Res* **15**:4227s–4232s.
- Shepherd FA, Rodrigues Pereira J, Ciuchini T, Lin H, Hirsh V, Thongprasert S, Campos D, Maolekkoopiroj S, Smyth GT, Giacino R, et al. (2005) Erlotinib in previously treated non-small-cell lung cancer. *N Engl J Med* **353**:123–132.
- Sherr CJ (1994) G1 phase progression: triggering on cue. *Cell* **79**:551–555.
- Sherr CJ and Beach D (1999) CDK inhibitors: Positive and negative regulators of G1-phase progression. *Genes Dev* **13**:1501–1512.
- Shin I, Ro J, Wu Y, and Arteaga CL (2005) Phosphorylation of p27<sup>KIP1</sup> at Thr-157 interferes with its association with importin  $\alpha$  during G1 and prevents nuclear export. *Biol Cell* **280**:6055–6063.
- Shin I, Yakes F, Rojo F, Lin N-Y, Bakin AV, Baselga J, and Arteaga CL (2002) p27<sup>KIP1</sup> nuclear import and cell cycle progression by phosphorylation of p27<sup>KIP1</sup> at threonine 157 and modulation of its cellular localization. *Nat Med* **8**:1145–1152.
- Singerling M and Pagano M (2000) Regulation of the Cdk inhibitor p27 and its deregulation in cancer. *J Cell Physiol* **183**:10–17.
- Tanaka K, Lee LM, Yoo KH, Lee SJ, Sun H, and Zhang H (1999) p27 (Kip1) ubiquitination and degradation is regulated by the SCF(Skp2) complex through phosphorylation of p27. *Curr Biol* **9**:661–664.
- Tsai H-C, Motti ML, Bruni P, Melillo RM, D'Alessio A, Califano D, Vinci F, Chiappetta G, Tschlis P, Bellacosa A, et al. (2002) Cytoplasmic relocation and inhibition of the cyclin-dependent kinase inhibitor p27<sup>KIP1</sup> by PKB/Akt-mediated phosphorylation in breast cancer. *Nat Med* **8**:1136–1144.
- Wang C, Hou X, Mohapatra M, Ma Y, Cress WD, Pledger WJ, and Chen J (2005) Activation of p27<sup>KIP1</sup> expression by E2F1, a negative feedback mechanism. *J Biol Chem* **280**:12339–12343.
- Weinberg RA (1995) The retinoblastoma protein and cell cycle control. *Cell* **81**:323–330.
- Yarden Y and Sliwkowski MX (2001) Untangling the ErbB signaling network. *Nat Rev Mol Cell Biol* **2**:127–137.
- Yaroslavskiy B, Watkins S, Donnenberg AD, Patton TJ, and Steinman RA (1999) Subcellular and cell-cycle expression profiles of CDK-inhibitors in normal differentiating myeloid cells. *Blood* **93**:2907–2917.

**Address correspondence to:** Dr. Roman Perez-Soler, Department of Oncology, Montefiore Medical Center, 111 East 210<sup>th</sup> Street, Hofheimer 100, Bronx, New York 10467. E-mail: rperezso@montefiore.org